Applied Thermal Engineering 111 (2017) 112–121

Contents lists available at ScienceDirect

Applied Thermal Engineering

journal homepage: www.elsevier.com/locate/apthermeng

Research Paper

An aspirating cooling system for regulating temperature of pyrolytic oven glass

D. Kumlutaş, Ö. Özer *, B. Eker, İ.D. Ünsalan

Mechanical Engineering Department, Dokuz Eylul University, Tınaztepe, Izmir, Turkey

HIGHLIGHTS

- Active suction cooling system of oven was modeled as a three dimensional using CFD.
- The aerodynamic design of the ASC system developed based on parametric studies.
- The maximum temperature at the oven door decreased 65 K by active cooling system.
- An extra 11.5 K cooling sustained at the pyrolytic oven door by parametric study.

ARTICLE INFO

Article history:
Received 1 April 2016
Revised 23 August 2016
Accepted 7 September 2016
Available online 8 September 2016

Keywords:
Computational fluid dynamics (CFD)
Household oven
Pyrolytic
Aspirating cooling system (ACS)

ABSTRACT

The aim of this study is to investigate the design parameter effects of an aspirating cooling system on the outer surface temperature of a household pyrolytic oven glass. Pyrolytic ovens include complicated components, such as an oven door, a cross-flow fan and an aspirating cooling system, and their complex interactions should be investigated in detail. In this study, the oven door and cross flow fan and aspirating cooling systems were modeled as a three dimensional system using a computational fluid dynamics and heat transfer method to investigate the fluid flow and temperature distribution of outer surface of the oven door. The simulation model predicted the temperature distribution based on the cross flow fan speed, cross flow fan position and channel design of the aspirating cooling system. The numerical results were validated against results obtained from an experimental study. The computational results show that the rotational speed of the cross flow fan, the cross flow fan position and the channel design of the aspirating cooling system play important roles in affecting the outer surface temperature distribution of the oven glass of a pyrolytic oven.

1. Introduction

In the design of domestic ovens, one of the most important parameters is outer glass temperature, especially in pyrolytic-type domestic ovens. Pyrolytic ovens have a self-cleaning function during which the temperature inside of the oven is increased over 500 °C. When the temperature inside the oven reaches these values, any food residue and grime adhered to the walls is simply burned off. This feature provides great convenience for users. However, this high-temperature increase should be considered with regards to safety. The outer surface temperature of the oven should be reduced to a safe level not harmful to the environment and living beings. An aspirating cooling system (ACS) has been designed to reduce the temperature of the outer surface of the oven door. This system circulates air between panes through the door, thereby reducing the external surface temperature of the door by convective cooling. Here, the velocity of the suctioned air and the design of oven door are very important. If excessive cooling takes place, the temperature within the oven could decrease and affect the self-cleaning function. This would lead to low energy efficiency and performance of the door.

Rek et al. [8] examined a newer generation, multifunctional oven and modeled radiative, conductive, natural and forced convective heat transfer mechanisms. They investigated many parameters that influence conditions inside an oven, such as the shape and power capacity of heaters, fan rotor rotational speeds, the thickness and quality of insulation and the design of the oven doors. Shaughnessy and Newborough studied radiative heat transfer mechanism of the oven door [9]. They suggested a low-emissivity oven (LEO) provides an energy efficient alternative to a conventional domestic electric ovens. Abraham and Sparrow [1] developed an algebraic method for predicting the time-based temperature variation of a thermal load situated in an electrically

* Corresponding author.
E-mail address: ozgunozer@gmail.com (Ö. Özer).

http://dx.doi.org/10.1016/j.applthermaleng.2016.09.023
1359-4311/

heated oven. Mistry et al. [6] studied transient, natural convective heat transfer in ovens. A computer-aided design using computational fluid dynamics and heat transfer (CFDHT) modeling of an electric oven involves a three dimensional, unsteady, natural convective flow-thermal field coupled with radiative heat transfer. Mistry et al. [7] developed a CFDHT-based methodology to evaluate the performance of a domestic gas oven. Fahey et al. [2] studied cooling on circuit of the door of a pyrolytic oven. They used CFD and experimental techniques to understand the flow behavior of the oven. The CFD results were validated with experimental hot-wire velocity measurements. The study established an understanding on oven door's cooling circuit but they did not determine the effect of it or determine the design parameters. Verboven et al. [13] investigated forced convection in an oven using CFDHT methods. They compared their numerical results with experimental results. Smolka et al. [11] investigated forced convection inside a drying oven by using experimentally validated three dimensional CFDHT analyses. To improve the temperature uniformity within the oven cavity, they changed parameters, such as the rotational speed of the device fan, the effectiveness of the distribution gaps and the rate of heat generated by the electric heaters. Smolka et al. also changed configurations, such as the locations of the heaters, the fan and the fan baffle. Overall, they improved the temperature uniformity and validated the results with an experimental test of the modified prototype.

As mentioned in the literature, the CFDHT method has been successfully applied for revealing and understanding complex flow characteristics [3,4,12]. The three dimensional modeling of an oven is essential for determining the air-side flow and heat transfer characteristics. For the first time in the literature, an oven door and an ASC are modeled together as a whole three dimensional system. Therefore, in this study, an oven door, a cross flow fan (CFF) and an ACS were simultaneously introduced in a heat transfer and fluid flow analysis to determine the outer surface temperature distribution of the oven door. Before investigating the oven door and ASC together, the ASC was first independently modeled. The mechanical structures of the ASC were developed based on parametric studies. Then, the oven door and ASC were modeled together, and the flow field and the temperature distribution were investigated. The numerical results were validated by comparison with results obtained from experimental studies. To reduce the temperature on the oven door outer surface, the influence of the fan rotational speed was numerically investigated. The results of the parametric studies showed that the rotational speed of the CFF played an important role in regulating the outer surface temperature of the oven door.

2. Numerical study

A computer-aided design (CAD) model of an oven was taken from a white goods company for the numerical study. The CAD model of a pyrolytic oven assembly is shown in Fig. 1b. The oven has an ASC for decreasing the outer surface temperature of the oven door. Details of the ASC and oven door are shown in Fig. 1b and c, respectively. The top view of the system is given at Fig. 1d which also shows that the CFF is positioned symmetry plane of the oven.

As mentioned, the main purpose of the ASC is to actively cool the oven door by drawing air between glass panes. The air suction power was provided by the CFF, which was part of the ACS. The oven door consisted of a quadruple glass layer as shown in Fig. 1c. Air from the chimney of the oven could be circulated between these glass layers, and a plastic profile was used to hold the glass pane together.

The air volume model of the oven door and the ASC is shown in Fig. 2a. The "A" side shown in Fig. 2c is the inner cavity of the oven and the "B" side is the outside of the oven.

In the regular ovens without the ACS, the heat transfer from the outdoor surface occurs via natural convection and radiation. However in the ovens with ACS with suction, air suctioned reverse direction of the natural convection and this effects the heat transfer. The outdoor air volume is added to the analysis for investigating this phenomena. The height and the width of the air volume is selected equal to the ovens size. The depth of the out air volume is related with the diameter of CFF as Shih et al. [10] suggested in their study. After some analysis were done to see appropriate size,

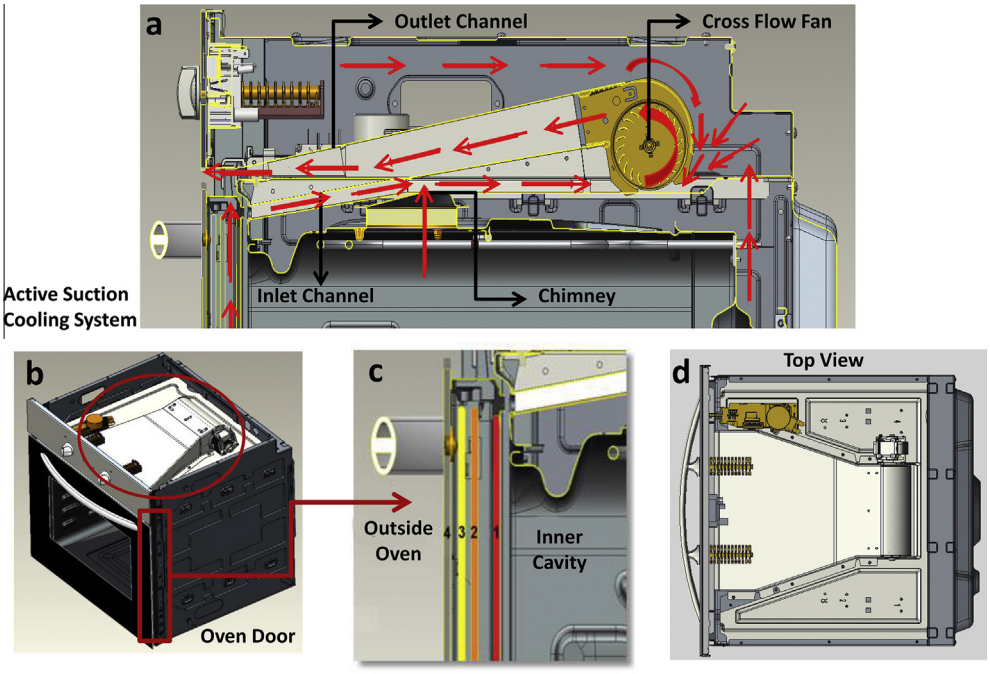

Fig. 1. Pyrolytic oven views (a) aspirating cooling system, (b) pyrolytic oven assembly, (c) oven door, (d) top view of oven.

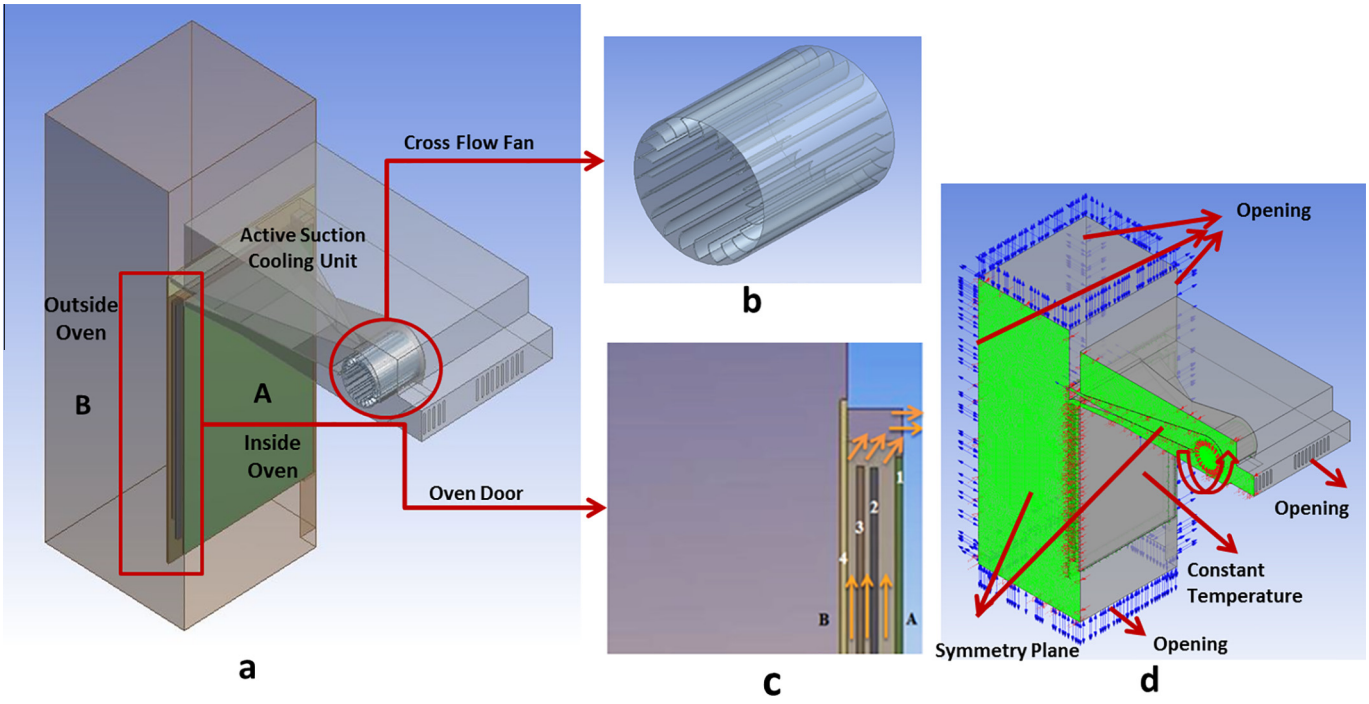

Fig. 2. Three dimensional air volume model (a) model of oven door and aspirating cooling system, (b) model of cross flow fan air, (c) model of oven door and air circulation of the oven, (d) boundary conditions of model.

the depth of outside air volume was determined to be three times the diameter of the CFF.

Glass number 1 (i.e., the eight inner glass panes) is the surface that contacts the oven inner cavity and glass number 4 (i.e., the outer glass pane) contacts the ambient atmosphere surrounding the oven. The structure of the ACS was prepared using a modeling program according to the CAD model of the oven with necessary simplifications and is shown in Fig. 2a. To prepare the ASC, the inlet and outlet channels, the chimney area and the fan were modeled. The system has two main bodies, which are the fan and the air cavity. A model of the CFF is shown in Fig. 2b. As seen from Fig. 2a, only half of the full oven door and ASC CAD were modeled because the air flow in the door was symmetrical.

To provide a realistic simulation, the CFDHT analysis generated a proper numerical grid model. The mesh structure of the system is shown in Fig. 3a. Because the thickness of the glass panes and the air gaps between the glass panes were small, the mesh element sizes were small for these regions. The body of the ambient air

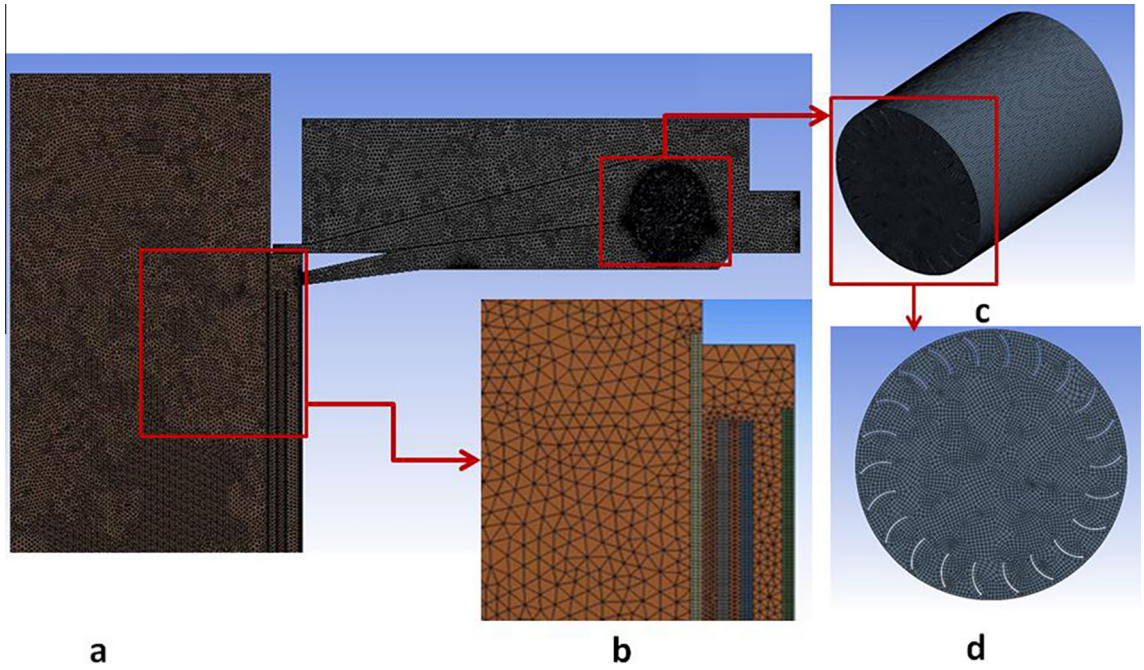

Fig. 3. Mesh details of the air volume model (a) mesh detail of oven door and aspirating cooling system, (b) mesh detail of oven door, (c) mesh detail of fan, (d) front view of fans' mesh detail.

Table 1
The study of determining optimum mesh model.

Case	Number of elements	Temperature at outer surface (K)
Case 1	3,436,288	324.31
Case 2	5,273,651	322.25
Case 3	10,285,361	322.31
Case 4	30,224,854	322.66

volume of the rest of door was meshed normally as shown in Fig. 3b. Fins of the CFF were very small compared with the air cavity. Overall, different domains meshed with different element sizes. The mesh details of fan are shown in Fig. 3c and d.

Different sizes of mesh elements was applied to the model and tried to find optimal number of elements for the final model. As it seen from Table 1 different number of mesh was applied to the CAD model. For comparing the cases average temperature of the outer surface of fourth glass were noted. Four models were prepared to see the effect of the number of elements. Even the model, which has the minimum number of elements and nodes (Case 1) having 1° accuracy. If the number of elements increases solver needs more time to get results but if number of elements is not enough model cannot validate the experimental results. If the other parameters that affect the CFD results are done properly, to get best converging results meshing process needs more time to spend on. Case 2 was chosen for this study as a final model. The final mesh structures of the oven door and ASC and is shown in Fig. 3.

After preparing the mesh, the boundary conditions of the model were defined. The air in the oven door and the ACS, the glass panes and the plastic profile were set as stationary domains whereas the fan was set as a rotating domain. The rotating speed of the CFF was set at 2400 rpm (which was further investigated in the parametric part of this study). The entrance and exit of the inlet and outlet channels, respectively, of the ACS and the chimney surface were defined as openings.

The outer surfaces of the air model exposed to the ambient atmosphere were defined as open boundary conditions. The necessary symmetry planes of all bodies were also set at the required boundaries. The remaining faces which were not openings or symmetry planes were assigned as no slip boundaries. The ambient, opening temperature was defined at 25 °C. The main heat transfer mechanism on the outside of the oven door was set as natural convection. As mentioned earlier, previous studies have compared different radiation models Mistry et al. [6]. However, no major differences in calculated temperatures have been reported based on these different models. Therefore, a surface-to-surface radiation model was selected for this study due to more rapid model convergence. Furthermore, k-epsilon turbulence model was selected for this study. Temperature values obtained from these previous experiments were used to define the first glass inner surface that intersected with the inner cavity of the oven. The previous experimental studies were performed when the systems were in thermal balance. Therefore, the numerical modeling of the current study were performed at steady state. The boundary conditions of model were shown in Fig. 2d.

3. Validation of CFD results

3.1. Fluid flow verification

To validate the velocity field of the ASC, velocity measurement tests were performed and compared with the CFD analysis. In the experiments, eleven of sixteen hot wire anemometers were placed on the air flow inlet of the ACS. The remaining anemometers were placed on the air flow outlet. The positions of the anemometers for

Fig. 4. Arrangement of anemometers in experimental study.

the velocity measurements of the ASC are shown in Fig. 4. When the system reached a steady state, air flow data were recorded every 0.3 s over the duration of approximately five minutes. After completing the experiments, the average flow data over the entire inlet and over the entire outlet were obtained to validate the numerical results.

The CFD results are shown in Fig. 5. The fluid flow velocities of the ACS and the oven door are shown in Fig. 5a and b.

The average velocity of the air at the suction opening in the ACS was 2.98 m s^{-1}. The average velocity at the outlet of ACS was 6.92 m s^{-1}. The differences between the experimental and numerical studies are shown in Table 2. The numerical results are similar to the experimental results, i.e., the CFD model was validated by the experimental study for these simulated conditions.

3.2. Temperature distribution verification

The CFDHT results were validated and compared with experimental results. A temperature experiment was performed during the pyrolytic cycle of 1.5 h. For all experiments, the ambient temperature was set at 25 °C. The surface temperature of the outer glass door was measured by a digital infrared thermometer which has 0.5% accuracy three minutes prior to the completion of the cycle. In addition, the surface temperature distribution was obtained via the thermal camera which has Thermal sensitivity < 30 mK. The temperature data obtained by the thermal camera and digital thermometer were used to validate the numerical study.

Fig. 6a shows the temperature distribution of the outer surface of the oven door in the experimental study. The measured temperature values (i.e., T1, T2,...,T12) were reported as the maximum temperatures values of the area (Fig. 6a). In the numerical study, the temperature distribution of the outer surface of the oven door is shown in Fig. 6b.

Table 3 shows a comparison of the experimental and numerical results. The maximum error in the analysis is noted as 15 K which is a point vise error. The maximum relative error between the temperature and analysis data was 4.42%. The relative error values ranged from 0 to 4.42%.

A scatter plot comparing the numerical and experimental temperature data is shown in Fig. 7. Both data sets were similar. This shows that the oven door and ASC can be modeled using the numerical study to estimate parametric values.

4. Parametric study

4.1. Effects of position of the CFF

The structure of the CFF with an impeller, a back wall, a vortex wall and a motor is shown in Fig. 8.

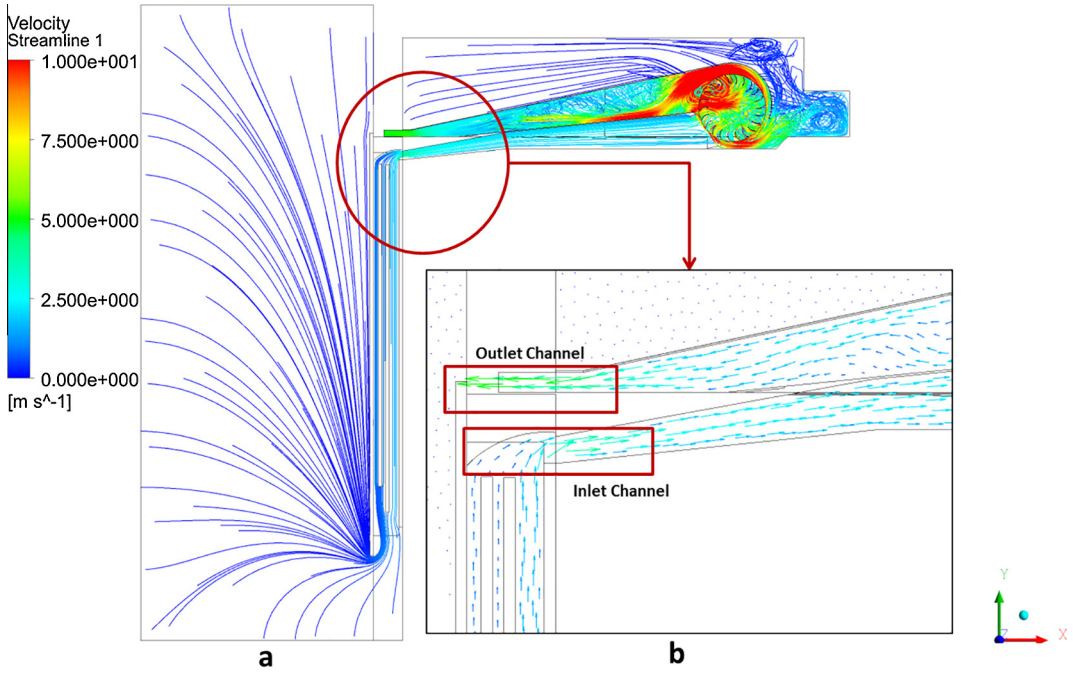

Fig. 5. Fluid flow of CFD study (a) ACS and oven door, (b) details of the inlet and outlet ACS.

Table 2
Comparison of the computational and the experimental study for the inlet and outlet channel of ASC unit.

Average velocity (m/s)	Experimental study	Numerical study	Absolute difference
Inlet	3.07	2.98	0.09
Outlet	7.78	6.92	0.86

As a priority in the numerical study of ACS, the optimum position of the CFF was determined based on operational principles. Depending on this position, the design parameters and positions of the inlet and outlet channels of the ACS were determined according to the literature and the limits of mechanical construction. The three dimensional air volume model of the ACS was prepared for CFD analyses. A air volume model of a first ACS design is shown in Fig. 9a and b. The first model examined whether a lower suction inlet channel design was effective, depending on the location of the CFF.

Table 3
Temperature comparison between experimental and computational results.

Temperature of test data	Experimental results (K)	Numerical results (K)	Error (%)
T1	343	358	4.37
T2	330	334	1.21
T3	325	338	4.00
T4	317	321	1.26
T5	312	312	0.00
T6	320	331	3.44
T7	321	321	0.00
T8	311	312	0.32
T9	317	331	4.42
T10	352	358	1.70
T11	332	334	0.60
T12	324	338	4.32

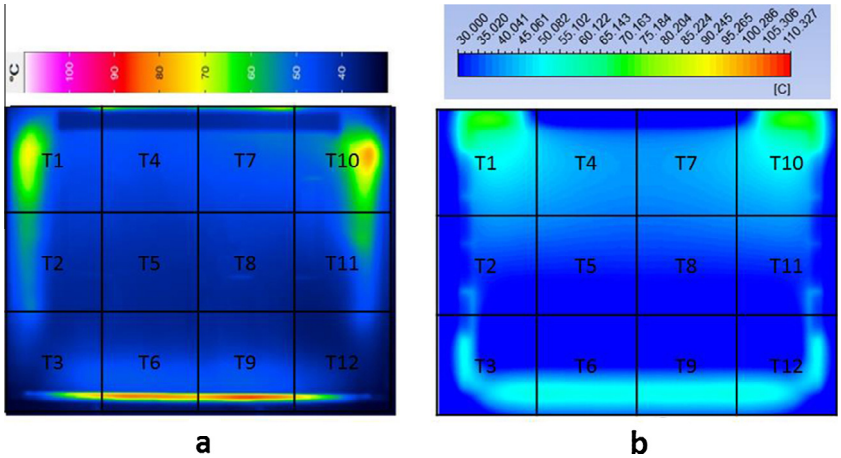

Fig. 6. The temperature distribution of the outer surface of oven door (a) experimental results, (b) computational results.

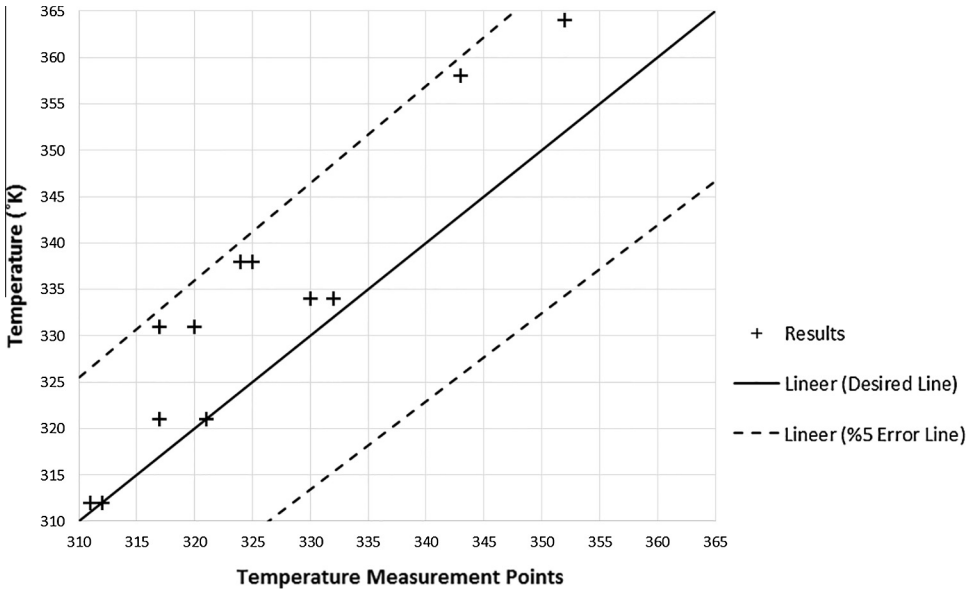

Fig. 7. Scatter plot comparing the numerical and experimental temperature data.

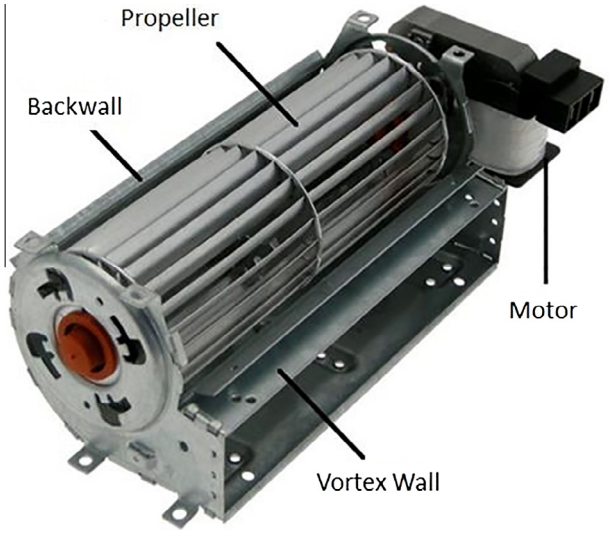

Fig. 8. Mechanical construction of CFF.

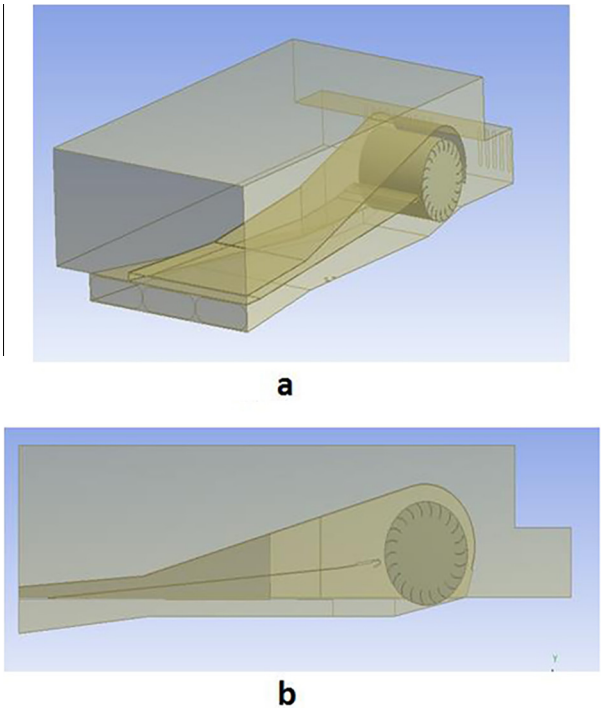

Fig. 9. (a) Air volume model of ACS, (b) cross-sectional view of ACS air volume model.

Three different CFF locations were investigated. The simulation results of the different locations of the CFF are shown in Fig. 10a–c.

As shown in Fig. 10a–c, the optimal velocity distribution was observed for the CFF location represented in Fig. 10c. Based on these numerical studies, the position of the inlet channel was located 5 mm from a tangent to the CFF blades.

In addition to this improvement, to maintain an airflow balance, which is suctioned from behind the CFF and from the oven door, the back wall design was studied. To determine the optimum angle (Ø) and sizes of the back wall (P1, P2) parametric studies were performed. Fig. 11a shows pressure contours of the ACS around the CFF. Fig. 11b shows a schematic view of the working principle of the CFF.

As a result of the numerical studies, the optimum angle and size of the back wall were determined. The design input parameters (P1, P2 and Ø) and corresponding suction channel inlet velocity are shown in Table 4.

As shown in Table 4, the maximum velocity of the suction channel was observed for DP 6. If the inlet velocity of the channel increased, the average temperature of the outer surface of the oven door decreased. Thus, for the back wall design, the parameters that defined model DP 6 was selected.

4.2. Effects of design of the upper blowing channel

After determining optimum CFF position and the angle and size of the back wall adjacent to the CFF, the upper blowing outlet channel was investigated. The entry area (i.e., the CFF fan outlet) was fixed, and the output area (i.e., just outside the mouth opening of the outlet channel) was varied, as shown in Fig. 12a and b.

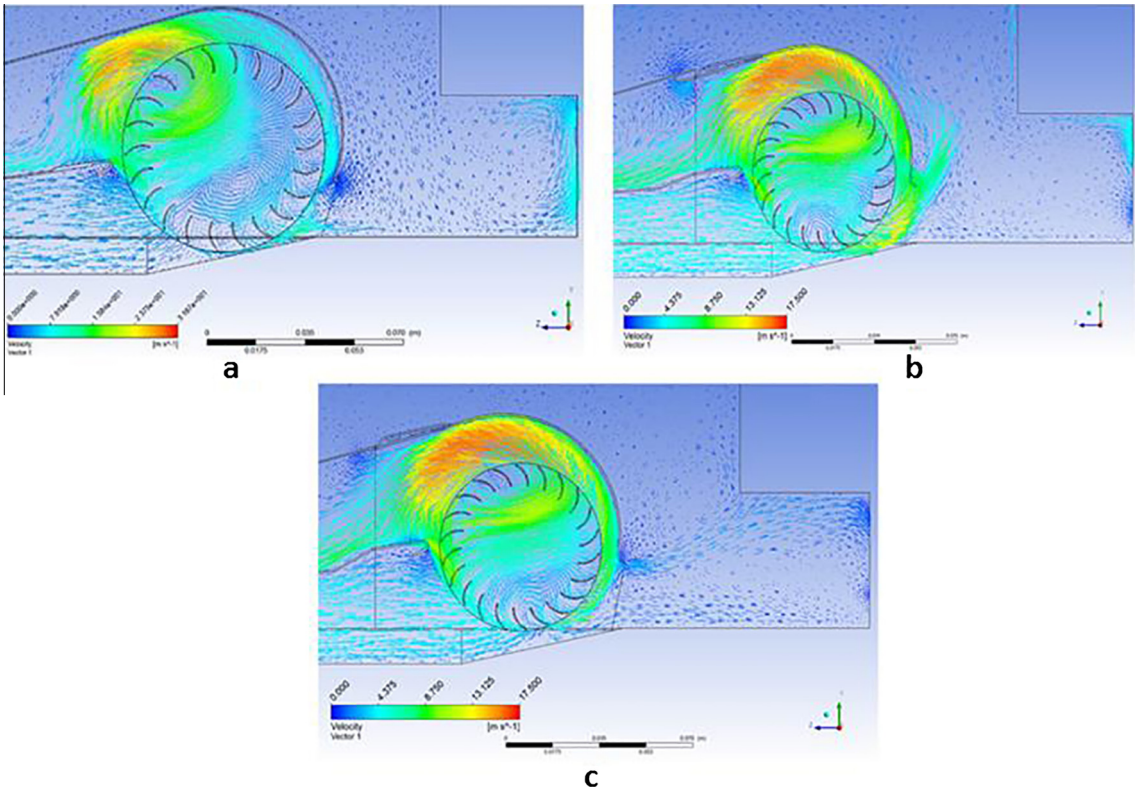

Fig. 10. Velocity vectors of ACS (a) inlet channel and CFF tangent, (b) back wall 2.5 mm from CFF, (c) back wall move away 5 mm from CFF.

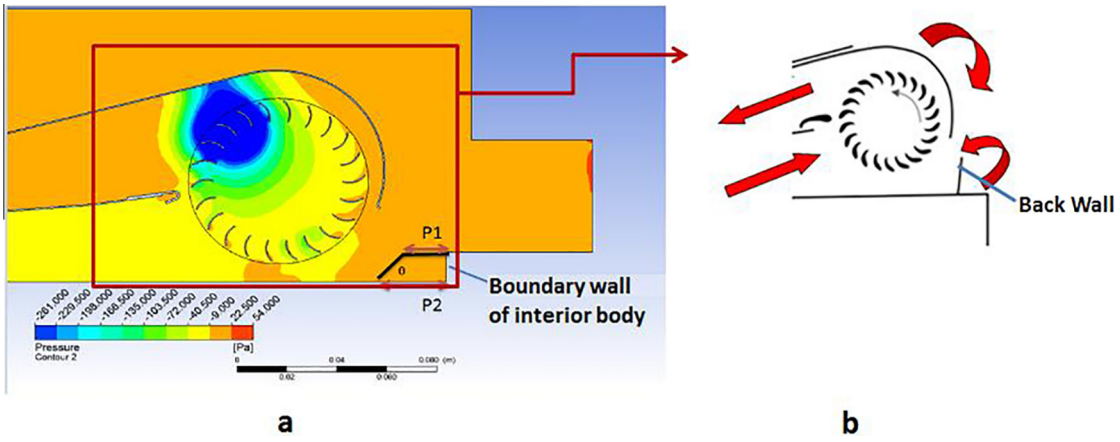

Fig. 11. The optimum positioning of the inlet channel depending on the boundary wall of interior body (a) pressure contours of ACS, (b) schematic view of CFF.

Table 4
Variations of velocity due to sizes and angle of back wall.

	P1 (mm)	P2 (mm)	Ø (°)	Inlet velocity of the suction channel (m/s)
DP 0	10	20	53.67	2.88
DP 1	15	25	52.27	1.95
DP 2	10	15	68.85	2.49
DP 3	10	25	40.73	2.44
DP 4	5	10	68.85	2.77
DP 5	7.5	15	59.88	2.79
DP 6	7.5	20	45.96	2.98
DP 7	7.5	25	36.46	2.74

Depending on parametric studies, the optimum value of the outlet channel blowing area was determined. The parameters of the upper blowing channel are shown in Table 5.

There was no noticeable pressure difference between the different designs as shown in Fig. 13. When horizontal dimension A was 10 mm and horizontal dimension B was increased from 60 mm, the

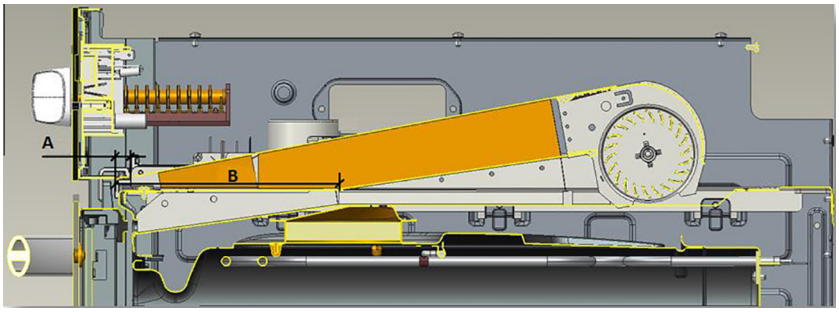

Fig. 12. The structure of upper blowing channel.

Table 5
Design data of upper blowing channel.

Design points	A (mm)	B (mm)	Pressure of outlet channel (Pa)	Design points	A (mm)	B (mm)	Pressure of outlet channel (Pa)
P1	100	20	0.00361700	P14	35	25	0.00292787
P2	90	100	0.00361645	P15	40	50	0.00289826
P3	100	100	0.00355916	P16	30	60	0.00288071
P4	80	90	0.00334849	P17	20	25	0.00285925
P5	60	100	0.00325768	P18	30	70	0.00283898
P6	70	80	0.00323822	P19	15	20	0.00278477
P7	60	70	0.00322628	P20	20	10	0.00275407
P8	60	60	0.00322119	P21	10	20	0.00274435
P9	100	60	0.00318347	P22	20	20	0.00274428
P10	50	60	0.00312891	P23	20	60	0.00273204
P11	60	20	0.00309237	P24	20	50	0.00270971
P12	25	15	0.00303135	P25	20	70	0.00261756
P13	25	35	0.00295115	P26	10	60	0.00234585

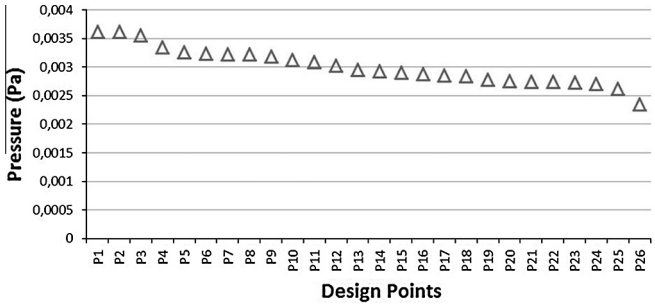

Fig. 13. Pressure comparison between design points of upper blowing channel.

resulting differences in pressure values were negligibly small. Due to the physical constraints of the channel, dimension A was set at 10 mm and dimension B was set at 150 mm.

After the parametric studies, validation experiments were performed and compared with the CFD analysis. An initial model was verified by an experimental study before continuing with the parametric numerical studies. A final ACS prototype was developed, and the experimental studies were repeated. The results of the numerical studies of the initial and final models are shown in Table 6.

Following these parametric studies, the ACS and the fluid flow of the system were improved. The average velocities of the airflow at the inlet (suction) and the outlet (discharge) of the ACS were increased by 40.8% and 17.02%, respectively. As the velocity increased, the outer surface temperature of the oven door decreased.

Table 6
Velocity comparison between first and final model of ASC system.

	Outlet	Inlet
First model	5.91 m/s	2.18 m/s
Final model	6.92 m/s	3.07 m/s
The rate of increase	17.02%	40.8%

4.3. Effect of rotational speed of CFF

At the oven door, heat is transferred by conduction, convection and radiation. In the oven cavity, the air is heated by heaters and circulates in the oven. In pyrolytic ovens, radiation is the dominant heat transfer mechanism because of the high temperatures. Radiation emitted by the heaters causes the door air cavity to heat up. The active suction system cools down the door cavity by convection. To determine the effect of the CFF rotational speed, the Reynolds number of the airflow was calculated according to Eqs. (4.1) and (4.2) [5]. The Reynolds number was based on the rotational speed of fan (n; rpm), the impeller external diameter (D; mm), the length of the blade chord (cp; mm) and the kinematic viscosity (v; $m^2\ s^{-1}$).

$$Re = \frac{U_L \cdot C_p}{v} \tag{4.1}$$

$$U_L = \frac{2 \cdot \pi \cdot n}{60} \cdot \frac{D}{2} \tag{4.2}$$

Fig. 14 shows the effect of the Reynolds number (*Re*) on the surface temperature of the oven door. The first vertical axis shows the average outer surface temperature (K) of the oven door, and the second vertical axis shows the average velocities (m/s) of the inlet and outlet channels. The horizontal axis shows the Reynolds number.

The increase of the Reynolds number depends on the fan rotational speed. As shown in Fig. 14, a minimum temperature was acquired when *Re* was 8540. Above a *Re* of 4880, there were no noticeable effects on the outer surface temperature of the oven

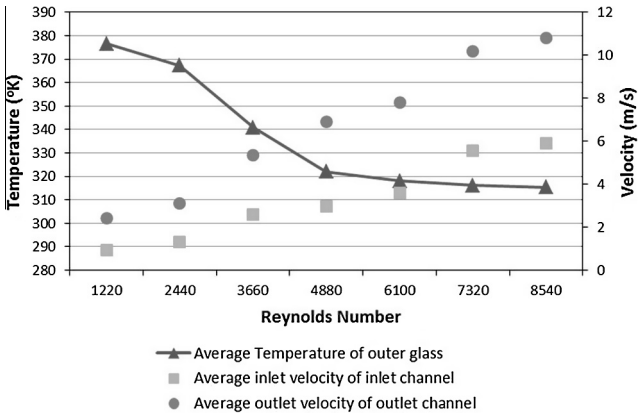

Fig. 14. The effect of speed of the cross flow fan on the outer surface of oven door.

door. However it must be noted that the Reynolds Number also related other parameters such as fan cord length. These parameters may have an additional effects on the flow characteristics.

4.4. The cumulative effects of parametric studies on ACS to the surface temperatures

As a final evaluation of this study, 3 prototype oven compared experimentally. The first model was the oven without ACS, the second one was the early prototype with ACS before CFD study and the last one was the oven design with ACS enhanced with the parametric study on this paper. The half of the oven door separated into 12 areas and the maximum temperatures in these areas are noted both with infrared camera infrared thermometer. "L" represents the total width of the oven door and X = 0 represents the mid area. The half oven doors surface temperature distributions at the pyrolytic stage are given in Table 7.

The results show that even the ACS without design optimization reduces the average surface temperature of the oven 13.25 K. Also the maximum temperature of the oven door decreased 48 K. As the temperature distributions of the prototype 1 and prototype 2 inspected, it can be noted that the major reduction takes place at the center areas. The reason of this situation is the CFF length is shorter than the oven door (can be seen in Fig. 1d) and air suctioned from the CFF is not enough to effect the sides.

After the parametric study, the suctioned air average velocity increased 40.8% as mentioned. This caused an extra 12 K reduction on the average temperature of the oven door in respect to Prototype 2 and 25.25 K reduction in respect to Prototype 1. The maximum temperature of the prototype 3 is 65 K less then Prototype 1. The temperature distribution of the prototype 3 is also more homogeneous due better use of the air channel between the oven door glasses.

5. Conclusions

The aim of this study was to investigate the heat transfer and fluid (air) flow characteristics of domestic ovens with aspirating cooling system (ACS) systems by implementing numerical methods. A prototype pyrolytic domestic oven was used. In the literature, numerical and experimental studies have been conducted for measuring the heat transfer and air flow inside oven cavities and within oven doors. The oven door and its upper fan provide active air suction from the door and were modeled using a computational fluid dynamic and heat transfer (CFDHT) method. The numerical results were validated by comparing with results obtained from experimental tests. In the literature, only a few studies have observed the heat transfer mechanisms of the oven door. A combined oven door and ACS was modeled in three dimensions, and parametric studies were performed. First, the ACS was modeled, and fluid flow was investigated. Based on these parametric studies, a new ACS model was developed with optimized CFF position and ACS channel geometry. After improving the ACS, the oven door and ACS were modeled together, and the outer surface temperature distribution of the oven door was investigated. Furthermore, the airflow Reynolds number was parametrically investigated.

The computational results show that the designs of ACS channels, the CFF position and the rotational speed of CFF play important roles on the outer surface temperature distributions of the oven door and the flow fields of the ACS. These predictions are proven by experimental comparison of these models. The maximum temperature of the oven door decreased 65 K and the average temperature decreased 25.25 K in respect to the oven without ACS.

These results shown that ACS can strongly reduce the surface temperature at the oven door which enables to design cool touch ovens even in the pyrolytic function where the inner temperature of the oven reach about 723 K.

It must be noted that these results can be improved by increasing the number of the design parameters such as the diameter of the CFF and the positions of the oven door glasses. Also it must be taken to the consideration that the investigated flow structures include laminar, turbulent and transition regions therefore slight changes of design parameters may significantly affect the results.

The ongoing researches also showed enhancement of the materials also has strong effect on the surface temperature. However the aerodynamic design must be revised according to these properties. For decreasing the solution time, artificial intelligence algorithms such as artificial neural networks may be also integrated to the solution method for the future studies.

Acknowledgements

This work was supported by The Scientific and Technological Research Council of Turkey (project grant no. TEYDEB 3130615). We gratefully acknowledge this support.

Table 7
Surface temperature distributions obtained from the comparison experiments (°C).

Prototype 1 (without ACS)			Prototype 2 (with ACS, before optimization)			Prototype 3 (with ACS, after optimization)		
X = 0	X = L/4	X = L/2	X = 0	X = L/4	X = L/2	X = 0	X = L/4	X = L/2
92	130	82	81	77	71	61	60	47
70	75	86	49	52	82	40	43	65
52	57	72	44	45	80	38	37	52
53	50	48	37	37	53	45	40	42
Average		72,25	Average		59	Average		47
Maximum		130	Maximum		82	Maximum		65

References

[1] J.P. Abraham, E.M. Sparrow, A simple model and validating experiments for predicting the heat transfer to a load situated in an electrically heated oven, J. Food Eng. 62 (2004) 409–415.

[2] M. Fahey, S.J. Wakes, C.T. Shaw, Use of computational fluid dynamics in domestic oven design, Int. J. Multiphys. 1 (2008) 37–57.

[3] Y. Fan, T. Hyde, N. Hewitt, P.C. Eames, B. Norton, Comparison of vacuum glazing thermal performance predicted using two-and three-dimensional models and their experimental validation, Sol. Energy Mater. Sol. Cells 93 (2009) 1492–1498.

[4] S. Ganapathisubbu, S. Dey, P. Bishnoi, J.L. Castillo, Modeling of transient natural convection heat transfer in electric ovens, Appl. Therm. Eng. 26 (2006) 2448–2456.

[5] L. Lazzarotto, A. Lazzarotto, A.D. Martegani, On cross-flow fan similarity: effects of casing shape, J. Fluids Eng. 123 (2001) 523–531.

[6] H. Mistry, S. Ganapathi-subbu, S. Dey, P. Bishnoi, J.L. Castillo, Modeling of transient natural convection heat transfer in electric ovens, Appl. Therm. Eng. 26 (2006) 2448–2456.

[7] H. Mistry, S. Ganapathisubbu, S. Dey, P. Bishnoi, J.L. Castillo, A methodology to model flow-thermals inside a domestic gas oven, Appl. Therm. Eng. 31 (2011) 103–111.

[8] Z. Rek, M. Rudolf, I. Zun, Application of CFD simulation in the development of a new generation heating oven, Strojniški vestnik – J. Mech. Eng. 58 (2012) 134–144.

[9] B.M. Shaughnessy, M. Newborough, Energy performance of a low-emissivity electrically heated oven, Appl. Therm. Eng. 20 (2000) 813–830.

[10] Y.C. Shih, H.C. Hou, H. Chiang, On similitude of the cross flow fan in a split-type air-conditioner, Appl. Therm. Eng. 28 (2008) 1853–1864.

[11] J. Smolka, A.J. Nowak, D. Rybarz, Improved 3-D temperature uniformity in a laboratory drying oven based on experimentally validated CFD computations, J. Food Eng. 97 (2009) 373–383.

[12] N. Therdthai, W. Zhou, T. Adamzack, Three-dimensional CFD modelling and simulation of the temperature profiles and airflow patterns during a continuous industrial baking process, J. Food Eng. 65 (2004) 599–608.

[13] P. Verboven, N. Scheerlinck, J.D. Baerdemaeker, B.M. Nicolaï, Computational fluid dynamics modelling and validation of the isothermal airflow in a forced convection oven, J. Food Eng. 43 (2000) 41–53.